Generalization of the Rabi population inversion dynamics in the sub-one-cycle pulse limit

N. Došlić
Department of Physical Chemistry, R. Bošković Institute, Bijenička 54, 10000 Zagreb, Croatia
(Received 17 March 2006; published 13 July 2006)

We consider the population inversion in a two-level system generated by a sub-one-cycle pulse excitation. Specifically, we explore the effect that the time derivative of the pulse envelope has on the Rabi dynamics. Our analysis is based on a combination of analytical, perturbative, and nonperturbative treatments and is complemented by numerical simulations. We find a shortening of the Rabi inversion period and show that complete inversion is unobtainable under resonant, ultrashort pulse conditions. The impact of nonresonant and carrier-envelope phase-dependent effects on the dynamics of two-level and multilevel systems is studied numerically, and conditions for complete population inversion are derived.

DOI: 10.1103/PhysRevA.74.013402 PACS number(s): 42.50.Hz, 32.80.Qk

I. INTRODUCTION

In the last decade ultrashort laser pulses consisting of only few oscillation cycles of the electromagnetic field [1,2], have been the topic of rapidly growing experimental and theoretical [3–6] interest. This intense activity is the result of both the exciting science and the vast range of possible applications [7–12].

Compared to traditional many-cycle laser pulses, few-cycle pulses are characterized by a very rapid onset and a fast variation of the laser electric field. As the duration of a few-cycle pulse, t_p, is comparable to the oscillation period of the carrier light, $t_p \leqslant T=2\pi/\omega$ they are also referred as ultrashort, irrespectively of their absolute duration in time [1]. In addition to the amplitude and carrier frequency, to fully characterize the electric field of an ultrashort laser pulse one needs to know the carrier-envelope (CE) phase, i.e., a shift that the carrier wave has with respect to the pulse envelope maximum [4]. In an interaction with a material system the strong dependence of the electric field on the CE phase gives rise to CE phase sensitive dynamics which has been observed across the electromagnetic spectrum. In the context of high order harmonic generation, for example, it has been shown that the temporal evolution of the emitted attosecond pulses directly depends on the CE phase of the femtosecond driving pulse [7,13,14]. Similarly, a strong CE phase dependence has been observed in the ionization of rubidium Rydberg atoms by few-cycle nanosecond radio-frequency pulses [15], while an extreme case of phase sensitivity has been demonstrated in the laser control study of the HCN→HNC isomerization reaction [16,17]. Uiberacker and Jakubetz have shown that only infrared (IR) pulses having a positive lobe followed by a negative lobe can induce a pump-dump motion of the wave packet that steers the system in the desired direction. In a driven two-level system, however, the phase dependence of the population inversion emerges only in the nonlinear field regime [18], suggesting that the CE phase-dependent dynamics arises in the interaction of a few-cycle pulse with a multilevel system.

While most of the theoretical research on ultrashort pulse dynamics has focused on CE phase effects, the sudden onset of the electric field in such pulses gives rise to a variety of interesting phenomena. Our goal in the present work is to investigate these phenomena and, in particular, the effects that the time derivative of the pulse envelope has on the population inversion dynamics of a two-level and a multilevel quantum system. In doing so we refine previous numerical studies [16,17,19,20] and extend the formalism of the Rabi dynamics [21–24] into the ultrashort pulse domain where simple assumption of an electric field consisting of a time-dependent envelope and a carrier wave are not any more valid [1].

The outline of the work is as follows. First the theory of a multilevel system interacting with a laser field is presented in a form suitable for describing the interaction with a sub-one-cycle laser pulses and the pulse form is subsequently specified. The main results are presented in Sec. IV, where we focus on the changes occurring in the dynamics of a two-level system in the sub-one-cycle pulse limit. The results are given both in the perturbative and nonperturbative approximation. Section V complements the theoretical analysis with numerical results that extend our conclusions beyond the two-level system. The final section contains a summary, conclusions, and an outlook for future research.

II. GENERAL THEORY

The time-dependent Schrödinger equation describing the dynamics of a system with dipole moment $\mu(\vec{r})$ interacting with the electromagnetic field reads

$$i\hbar\frac{\partial}{\partial t}\Psi(\vec{r},t)=\left[H_0(\vec{r})+\frac{\mu(\vec{r})}{c}\frac{\partial A(t)}{\partial t}\right]\Psi(\vec{r},t), \tag{1}$$

where $H_0(\mathbf{r})$ is the unperturbed Hamiltonian of the system and $A(t)$ is the vector potential

$$A(t)=-\frac{F_0 c}{\omega}m(t)\sin(\omega t+\phi) \tag{2}$$

having a bell-shaped envelope $m(t)$. Accordingly, the electric field $E(t)$ is given by

$$E(t) = -\frac{1}{c}\frac{dA(t)}{dt} = F_0 m(t)\cos(\omega t + \phi) + \frac{F_0}{\omega}\frac{dm(t)}{dt}\sin(\omega t + \phi). \tag{3}$$

In the above equation the first term corresponds to a pulse with a cosine-oscillating carrier field, while the second term arises because of the finite pulse duration. In the sub-one-cycle pulse regime the impact of the time derivative of the pulse envelope, the so-called switching term, cannot be neglected. Also, the above formulation assures that the electric field $E(t)$ is a solution of the Maxwell equations in the propagation region [25]. In such case the field has a vanishing dc component [1,8]

$$\int_{-\infty}^{\infty} E(t)dt = 0. \tag{4}$$

Note that Eq. (1) is not generally valid, but it describes correctly the interaction with atomic or molecular systems for which the coordinate dependence of the vector potential can be neglected.

Equation (1) is solved by expansion of the time-dependent wave function $\Psi(\vec{r},t)$ in the set of stationary solutions of the isolated system $\psi_i(\mathbf{r})$; $i=1,2,\ldots,N$ with corresponding eigenenergies E_i

$$\Psi(\vec{r},t) = \sum_i a_i(t)\psi_i(\vec{r})e^{-iE_i t}. \tag{5}$$

The expansion coefficients satisfy the set of coupled equations

$$\frac{d}{dt}a_i(t) = -i\sum_j (V_{ij}^0 + V_{ij}^1)a_j(t), \tag{6}$$

where the matrix elements of V_{ij}^0 and V_{ij}^1 are given by

$$V_{ij}^0 = \frac{F_0\mu_{ij}}{2}m(t)[e^{i\omega_{ij}t}(e^{i(\omega t+\phi)} + e^{-i(\omega t+\phi)})] \tag{7}$$

and

$$V_{ij}^1 = \frac{F_0\mu_{ij}}{\omega}\frac{dm(t)}{dt}\frac{1}{2i}[e^{i\omega_{ij}t}(e^{i(\omega t+\phi)} - e^{-i(\omega t+\phi)})]. \tag{8}$$

In Eqs. (7) and (8) $\omega_{ij}=(E_i-E_j)/\hbar$, and μ_{ij} are the dipole matrix elements $\mu_{ij}=\langle i|\mu|j\rangle$. The form of the envelope $m(t)$ is application dependent and needs to be specified.

III. FEW-CYCLE PULSE CONSTRUCTION

Before analyzing the dynamics, we describe a procedure for constructing ultrashort laser pulses. The vector potential is assumed to have an envelope of the type

$$m(t) = \mathrm{sech}\left(\frac{t}{\alpha}\right), \tag{9}$$

with $\alpha_{1/2}=\alpha\ln(2+\sqrt{3})$ being the half-width of the pulse at half maximum. In the present work preference has been given to the sech-type envelope over the more widely used Gaussian type for analytical convenience. In other aspects the presented few-cycle pulse construction follows that of Uiberacker and Jakubetz [16]. In Eq. (6) the integration interval is $[-t_{max},t_{max}]$ and by imposing the condition $t_{max}=s_0\alpha$, $s_0\geqslant 6.5$ one ensures that on the ends of the interval the electric field is effectively zero. It is now convenient to express the width of the pulse in terms of the number of optical cycles of the carrier (n_c) that it contains

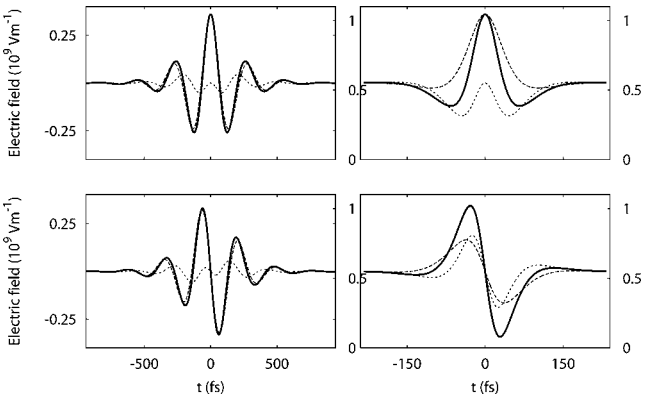

FIG. 1. 1.0-cycle (left) and 0.25-cycle (right) sech pulses with CE phases $\phi=0$ (upper) and $\phi=\pi/2$ (lower). The total electric field of the pulse (solid line) is compared to the pulse envelope with a cosine carrier field (dashed line) and to the time derivative of the pulse envelope with a sine carrier field (dotted line).

$$2\alpha = n_c T = n_c\frac{2\pi}{\omega}. \tag{10}$$

Clearly, ultrashort pulse conditions are achieved for $n_c<1$. The above relation, also, provides a link between the carrier frequency and the pulse duration.

Figure 1 shows the total electric field, as well as the two field components specified in Eq. (3) for a one-cycle and a quarter-of-cycle pulse with carrier frequency of $\omega=3.48$ THz and amplitude $F_0=0.36\times10^9$ V m^{-1}. The phases are $\phi=0$ and $\phi=\pi/2$ on the left and right panel, respectively. Hence, these pulses represent extreme examples of cosine and sine pulses. It is apparent that the time derivation of the envelope $m(t)$ (dotted line) has a negligible contribution to the total field strength of the one-cycle pulse, while it strongly modifies the shape of the 0.25-cycle one. Actually, in the later case the two field components have approximately the same magnitude. Moreover, sine pulses have a larger peak strength than the corresponding cosine pulse. The same is valid for the electric field component of the fluence $F_E=\int_{-\infty}^{\infty}E(t)^2dt$ which for sech-shaped pulses is given by

$$F_E = F_0^2\alpha\left(1+\frac{1}{3n_c\pi^2}\right) - \frac{F_0^2\alpha(1+n_c\pi^2)\cos(2\phi)\mathrm{cosech}(n_c\pi^2)}{3n_c}. \tag{11}$$

F_E has a sinusoidal behavior with maximum at $\phi=\pi/2$ which in the ultrafast limit $n_0\to0$ reduces to

$$\lim_{n_c\to 0} F_E = F_0\alpha^2\left(1+\frac{2\sin^2(\phi)}{3n_c^2\pi}\right). \tag{12}$$

Note, however, that the total fluence of the laser pulse is not phase dependent for it comprises the electric as well as the magnetic contribution which are shifted in phase by $\pi/2$.

IV. TIME-DEPENDENT SOLUTIONS FOR THE TWO-LEVEL PROBLEM

After specifying the form of an ultrashort pulse we consider its interaction with a two-level system. This simple case study allows us to understand the main changes in the dynamics occurring in the ultrashort pulse limit [21,22].

In the rotating wave approximation (RWA) Eq. (6) reads

$$\frac{d\mathbf{a}(\mathbf{t})}{dt} = -i\frac{F_0\mu_{12}}{2}\operatorname{sech}\left(\frac{t}{\alpha}\right)\begin{vmatrix}0 & 1\\ 1 & 0\end{vmatrix}\mathbf{a}(\mathbf{t}) - \frac{F_0\mu_{12}}{2\alpha\omega}\operatorname{sech}\left(\frac{t}{\alpha}\right)\tanh\left(\frac{t}{\alpha}\right)\begin{vmatrix}0 & 1\\ -1 & 0\end{vmatrix}\mathbf{a}(\mathbf{t}), \tag{13}$$

and can be most conveniently solved by introducing a new time variable, defined as

$$\tau = \int_0^t \frac{F_0\mu_{12}}{2}m(t)dt = F_0\alpha\mu_{12}\arctan\left[\tanh\left(\frac{t}{2\alpha}\right)\right]. \tag{14}$$

Strictly speaking, the RWA approximation should not be used in the ultrafast pulse regime, but, as it will be shown shortly by comparison with numerical solutions of Eq. (6), it is a valid approximation for a two-level system interacting with an IR pulse.

In terms of τ the set of equations for the coefficients $a(t)$ is

$$\frac{d\mathbf{a}(\tau)}{d\tau} = -i\begin{vmatrix}0 & 1\\ 1 & 0\end{vmatrix}\mathbf{a}(\tau) + \frac{4\omega\tau}{3F_0\mu_{12}n_c^2\pi^2}\begin{vmatrix}0 & 1\\ -1 & 0\end{vmatrix}\mathbf{a}(\tau) = -i\begin{vmatrix}0 & 1\\ 1 & 0\end{vmatrix}\mathbf{a}(\tau) + \kappa\tau\begin{vmatrix}0 & 1\\ -1 & 0\end{vmatrix}\mathbf{a}(\tau), \tag{15}$$

where in the derivation of the second term in the equation, the so-called switching term, $\kappa\tau$ we made a linear approximation to the coefficient of the second term in Eq. (13) in terms of τ. In the multicycle regime of light-matter interaction Eq. (15) reduces to a standard two-level system equation, while in the ultrashort regime the importance of the switching term rises quadratically with $1/n_c$. Note also that the term $F_0\mu_{12}$ in the denominator is contained in the definition of τ. Since Eq. (15) cannot be directly solved, approximate solutions are sought, either by using the perturbation theory or by transforming the system into an approximate second order differential equation.

A. Perturbative dynamics

We proceed by investigating a two-level system dynamics within the framework of the perturbation theory. Following the approach of Genkin [23,26] the quantity $u(\tau)=a_1(\tau)/a_2(\tau)$ is introduced in Eq. (15) and the system is converted into a single equation of the form

$$\frac{du(\tau)}{d\tau} = (i-\kappa\tau)u^2(\tau) - (i+\kappa\tau). \tag{16}$$

In the few-cycle regime κ is regarded as a small parameter, $\kappa \ll 1$, and presumably the solution $u(\tau)=u_0(\tau)+u_1(\tau)$ changes only slightly from the zeroth-order solution $u_0(\tau)$ given by

$$\frac{du_0(\tau)}{d\tau} = iu_0^2(\tau) - i. \tag{17}$$

The first-order correction is obtained by inserting Eq. (17) into Eq. (16) and retaining the linear terms in $u_1(\tau)$. In such a case the equation for $u_1(\tau)$ reads

$$\frac{du_1(\tau)}{d\tau} = [2iu_0(\tau) - 2\kappa u_0(\tau)\tau]u_1(\tau)^2 - \kappa\tau[1+u_0(\tau)^2]. \tag{18}$$

In the smooth switching regime the κ dependence in the homogeneous term can be neglected, and by introducing the solution of the zero-order problem the first-order correction is obtained as

$$u_1(\tau) = \kappa\tau\cot(\tau) + \frac{\kappa}{4}\cos(2\tau)\csc(\tau)^2. \tag{19}$$

In Eq. (19) the magnitude of $u_1(\tau)$ increases linearly in time indicating an efficient energy transfer. Obviously, such an increase cannot go on indefinitely because the perturbation theory fails, i.e., the above equation is restricted to short times and small switching parameters ensuring that the perturbation condition $|u_1/u_0| \ll 1$ is fulfilled. Accordingly, the level population dynamics is modified to

$$|a_1(\tau)|^2 = \frac{(u_0+u_1)^2}{1+(u_0+u_1)^2} \approx \cos^2(\tau)\left\{1+\frac{1}{2}\kappa^2\tau^2[1-\cos(2\tau)]\right\}. \tag{20}$$

Apart from the linear increase in time, the first-order correction to the population dynamics superimposes a function oscillating at twice the optical frequency to the $\cos(\tau)$ dynamics. In order to get a better physical insight into the changes of the frequency of Rabi oscillation due to the perturbation we rescale the time variable as $\tau \to \tau/\sqrt{(1-\kappa^2)}$. Equation (20) then reads

$$|a_1(\tau)|^2 \approx \cos(\sqrt{1-\kappa^2}\tau)^2\left\{1+\frac{1}{2}\kappa^2\tau^2[1-\cos(2\sqrt{1-\kappa^2}\tau)]\right\}, \tag{21}$$

where the term proportional to κ^4 has been neglected. Direct comparison with the numerical solution reveals that the shortening of the population inversion period is indeed a key feature of the dynamics in the ultrafast pulse limit.

B. Nonperturbative dynamics

In the nonperturbative approach the two-level system of Eq. (15) is transformed into an equivalent second-order dif-

ferential equation for the initial state coefficient $a_1(\tau)$,

$$-(1+\kappa^2\tau^2)a_1(\tau)+\frac{\kappa}{i+\kappa\tau}a_1'(\tau)-a_1''(\tau)=0. \quad (22)$$

For short pulses one can expand the factor in front of $a_1'(\tau)$ in a Taylor series around $\tau=0$ and by retaining only the first-order terms in τ obtain a more tractable equation of the form

$$-(1+\kappa^2\tau^2)a_1(\tau)-(i\kappa-\kappa^2\tau)a_1'(\tau)-a_1''(\tau)=0. \quad (23)$$

Clearly, the range of validity of the expansion depends on the magnitude of κ. The most critical parameter is n_c, the number of field oscillation in the width of the pulse that, for other parameters in the standard range for molecular isomerization ($F_0 \approx 5\times10^7-5\times10^8$ V m^{-1} and $\omega\approx 3-90$ THz), should be approximately $n_c \geqslant 0.5$. Equation (23) can be solved exactly by making the substitution $a_1(\tau)=u(\tau)v(\tau)$ and requiring that the terms in front of u' vanish, i.e.,

$$(i\kappa-\kappa^2\tau v u'+2v')u'=0.$$

This yields a simple differential equation for $v(\tau)$ with the solution

$$v=e^{-i\kappa(\tau+\tau_{max})/2+i\kappa^2(\tau^2-\tau_{max}^2)} \quad (24)$$

and a corresponding hypergeometric equation for $u(\tau)$ given by

$$\tfrac{1}{4}(f_0+f_1\tau+f_2\tau^2)u(\tau)+u''(\tau)=0, \quad (25)$$

where $f_0=4+3\kappa^2$, $f_1=2i\kappa^3$, and $f_2=\kappa^2(4-\kappa^2)$. The solution of the above equation reads

$$u(\tau)=e^{-[i(f_1\tau+f_2\tau^2)/4\sqrt{f_2}]}c_1H_\nu(z) + e^{-[i(f_1\tau+f_2\tau^2)/4\sqrt{f_2}]}c_{21}F_1\left(-\frac{\nu}{2};\frac{1}{2};z^2\right). \quad (26)$$

Here $H_\nu(z)$ is the Hermite function of order ν and argument z

$$\nu=\frac{if_1^2-4f_0f_2+8if_2^{3/2}}{16f_2^{3/2}}, \quad z=\frac{\left(\frac{1}{4}+\frac{i}{4}\right)(f_1+2f_2\tau)}{f_2^{3/2}},$$

and ${}_1F_1(-\nu/2;\frac{1}{2};z^2)$ is the Kummer confluent hypergeometric function. The normalization constants c_1 and c_2 can be readily calculated from the initial conditions $a_1(-\tau_{max})=1$, $a_1'(-\tau_{max})=0$ or, equivalently, from $u(-\tau_{max})=1$ and $u'(-\tau_{max})=-v'(\tau_{max})$. They also ensure that in the multicycle pulse limit Eq. (26) correctly approaches the cosinusoidal two-level-system dynamics. In contrast to the perturbative solution, the above solution does not lend itself readily to physical interpretations in terms of changes of the Rabi dynamics. However, the existence of a time independent component in the argument $z_{\tau_0}=(\frac{1}{4}+i/4)f_1/f_2^{3/2}$ indicates that complete population inversion is not possible. In the few-cycle regime, $n_c \geqslant 0.5$, the maximum depopulation of the ground state has been numerically estimated as $P_1^{min}\approx\kappa^2/4$.

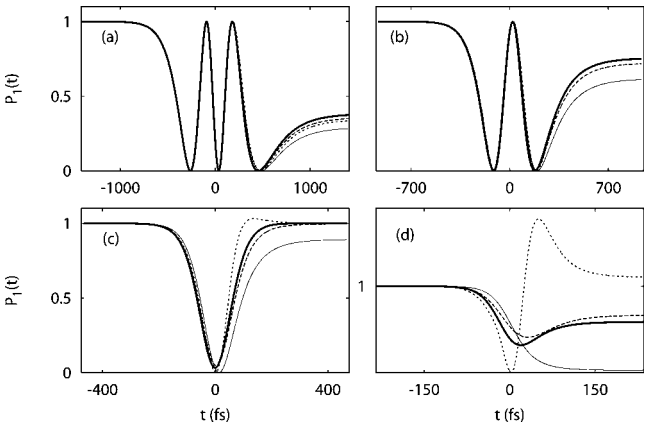

FIG. 2. Two-level system: Population evolution curves of the lower state interacting with (a) $n_c=1.5$, (b) $n_c=1.0$, (c) $n_c=0.5$, and (d) $n_c=0.25$. The numerical solution of Eq. (13) (solid, bold line) is compared to the analytical results: nonperturbative (long dashed), perturbative (short dashed), and multicycle (solid, thin line).

V. NUMERICAL RESULTS AND DISCUSSION

A. Resonant two-level system

The main goal of this section is to estimate the range of parameters for which the analytical results of previous sections are good approximations to the exact solution. It is also interesting to investigate the two-level system dynamics in extreme nonperturbative conditions, i.e., in the case of a very fast field switching regime. The numerical simulations are based on the solution of Eq. (13). The parameters of the two-level system correspond to the splitted ground state of acetylacetone (ACAC), a prototype intramolecular hydrogen bonded system. Specifically, the ground state doublet has a resonance frequency of $\omega_{12}=3.48$ THz and dipole matrix element of $\mu_{12}=-2.2$ D.

Figure 2 displays the population dynamics of the ground state interacting with laser pulses of decreasing durations, corresponding to the 1.5-, 1-, 0.5-, and 0.25-cycle pulses. The field amplitude is $F_0=0.36\times10^9$ V m^{-1}. The relatively strong field ensures that significant population transfer can be achieved even with the shortest pulse. The corresponding time-dependent electric fields for the 1.0- and 0.25-cycle pulses with $\phi=0$ are illustrated in the Fig. 1. Both analytical results, the perturbative (dotted line) and nonperturbative (dashed line) are contrasted to the numerical solution (solid, bold line) of Eq. (13) and to the population dynamics in the multicycle regime (thin line). In the upper panel of Fig. 2 (top) the population dynamics triggered by an interaction with longer pulses has been explored. For the 1.5- and 1-cycle pulses the four curves are virtually indistinguishable during the initial and middle part of the interaction, but differences among them emerge in the switchoff period at around $2\alpha=500$ fs. From the accuracy point of view both analytical results describe correctly the dynamics and are very close to the numerical solution. As expected, larger discrepancies in the dynamics occur upon interaction with the 0.50 and 0.25 pulses, as illustrated in the lower panel of Fig. 2. The switching parameters are $\kappa=-0.47$ and $\kappa=-1.9$ a.u.t.$^{-1}$ for the 0.5- and 0.25-cycle pulses, respec-

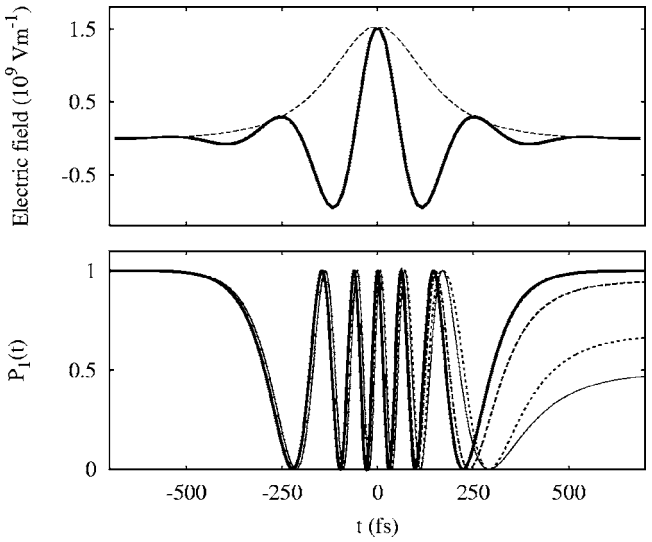

FIG. 3. Two-level system. Upper: Total electric field and pulse envelope of a resonant, $n_c=0.75$, $F_0=0.36\times10^9$ V m^{-1}, $\kappa^2/4=0.01$ pulse. Lower: The population inversion dynamics of the lower state. Numerical solution of Eq. (13) (solid, bold line) and analytical solutions: nonperturbative (long dashed), perturbative (short dashed), and multicycle (solid, thin line) are shown.

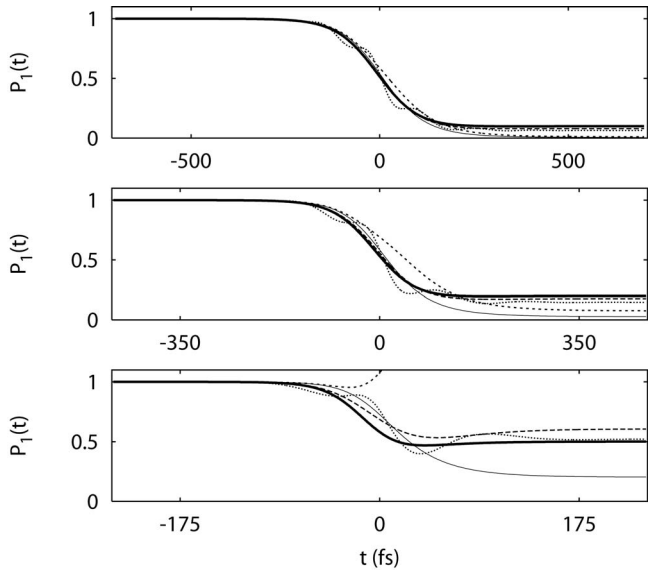

FIG. 4. Two-level system: Numerical optimization of the population inversion dynamics for (top) $n_c=0.75$, $F_0=1.28\times10^8$ V m^{-1}, (center) $n_c=0.5$, $F_0=0.18\times10^9$ V m^{-1}, and (bottom) $n_c=0.25$, $F_0=0.28\times10^9$ V m^{-1} pulses. Numerical RWA (solid, bold line) and non-RWA (dotted) solutions are shown together with analytical: nonperturbative (long dashed), perturbative (short dashed), and multicycle (solid, thin line) solutions.

tively. In this regime perturbation theory fails, while the nonperturbative analytical results hold well even in extreme nonperturbative conditions ($n_c=0.25$). Analyzing more closely the dynamics one sees that the switching term provides an additional drive to the system that manifests itself as a speedup of the population dynamics. The effect can be clearly seen form Fig. 3 where we have compared the population dynamics induced by a very strong 0.75-cycle pulse ($F_0=1.5\times10^9$ V m^{-1}). After a series of population inversions a time delay of $\approx$80 fs is observed between the exact and the cosinusoidal dynamics.

Next, it was natural to presume that a faster energy transfer encountered in the ultrafast pulse regime reduces the efficiency of a single population inversion event. In order to investigate such a possibility a series of numerical simulations with resonant 0.75-, 0.5-, and 0.25-cycle pulses have been performed. For each of the three cases the field amplitude F_0, in Eq. (13) has been optimized in such a way as to maximize the population transfer of the numerical solution. For that amplitude, the analytical, perturbative, and cosine curve have been computed and illustrated in Fig. 4. For completeness, the non-RWA solution, given in Eq. (6), is also shown. Evidently, as the number of oscillations of the carrier wave in the pulse width decreases, the onset of the electric field is faster and the efficiency of the population inversion decreases. The effect of the time derivative of the pulse envelope on the population dynamics is so large that it reduces the inversion efficiency of the 0.25-cycle pulse to 50%. Note that for the 0.75 and 0.5 pulses the estimate for the maximum depopulation of the ground state $P_1^{min}=0.09$ and $P_1^{min}=0.22$ finds good agreement with the numerical results. It goes without saying that for pure Rabi-type dynamics one can always construct a π-pulse which induces a complete population inversion. For sub-one-cycle pulses, however, a complete inversion is not possible under resonant conditions. In other words, the short duration of the pulse leads to the breakdown of the generalized π-pulse condition. To complement the above picture we shall consider nonresonant excitations, carrier phase effects, and multilevel dynamics.

B. Nonresonant two-level system

Let us first discuss the variation of the population inversion efficiency of the two-level system with respect to the carrier frequency and CE phase. The results have been obtained by numerical integrations of Eq. (6). The full form of the laser pulse is given in Eqs. (2) and (3) and the field amplitude is fixed to $F_0=0.27\times10^9$ V m^{-1}, which is the value at the onset of saturation for the pulse with CE phase and $n_c=0.25$ $\phi=0$. Figure 5 illustrates the variation in the final population of the upper state $|a_2(t_{max})|^2$. Two features are immediately noticeable: (i) the efficiency of the population inversion is almost independent on the CE phase, and (ii) a complete population transfer can be achieved by using nonresonant ultrashort laser pulses.

The phase sensitivity of the population inversion is related to the power spectrum $E(\omega)=\int_{-\infty}^{\infty}E(t)e^{i\omega t}$ of the laser field [18]. For the range of field parameters considered in this calculation the laser power spectra are not CE phase dependent. The weak oscillatory behavior of the upper state population probability landscape reflects the oscillations of the laser fluence as shown in Eq. (11). Indeed, in the range $5\times10^8<F_0<5\times10^9$ V m^{-1} numerical simulations carried out at constant fluence show complete insensitivity to the CE phase.

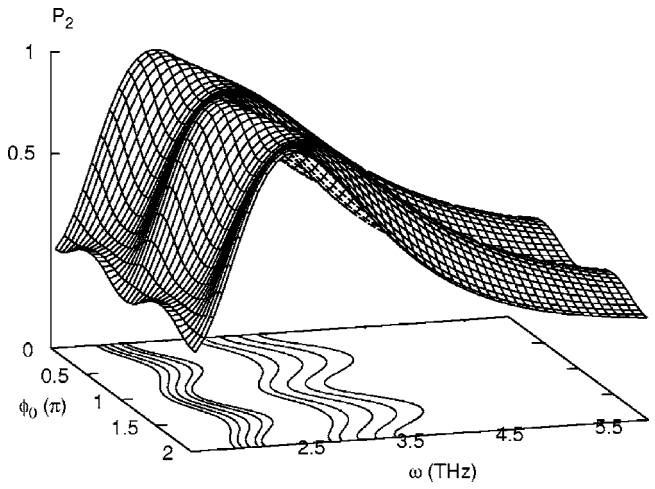

FIG. 5. Two-level system dynamics: Variation in the final population of the upper state with respect to the laser frequency and CE phase for $n_c=0.25$. The results are obtained by the numerical solution of the non-RWA Eq. (6). The resonst frequency is $\omega=3.48$ THz.

Secondly, a complete population inversion occurs at $\omega=2.40$ THz, thus at a value that is 1.08 THz redshifted from resonance. As the applied electric field of $F_0=0.27\times10^9$ V m^{-1} is not sufficiently strong to induce such a large ac Stark shift of the energy levels, the computed frequency shift must, therefore, be due to the changes in the laser pulse caused by the sudden onset of the field. Along this line, in Fig. 6 we have compared the amplitude of three laser fields. The first pulse is the maximum efficiency pulse with $\omega=2.40$ THz, while the second one is the resonant pulse with $\omega=3.48$ THz. The third pulse is resonant at $\omega=3.48$ THz, but the electric field of the pulse has been computed without taking into account the time derivative of the pulse envelope, i.e., the pulse form is simply given by $F_0\,\mathrm{sech}(t/\alpha)\cos(\omega t)$. Note that by adjusting F_0 the third pulse can actually become a π pulse that would induce a complete population transfer

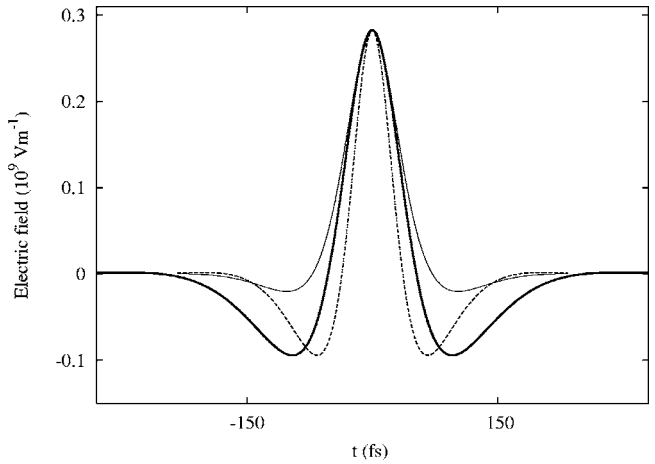

FIG. 6. Electric field of three sub-one-cycle pulses ($n_c=0.25$): nonresonant $\omega=2.40$ THz (solid line), resonant $\omega=3.48$ THz (dashed line), and resonant $\omega=3.48$ THz without the switching term (thin solid line).

in a many-cycle pulse regime. At the field maximum there is a streaking similarity between the off-resonant pulse and the simplified pulse, whereas the width of the "true" resonant pulse is much smaller. Obviously, the sudden onset of the field reduces the effective area of the pulse and the shift toward lower frequency is a mere compensation for that effect.

On this ground it is possible to compute the effective frequency of the laser pulse by equating the electric field of the pulse at shifted frequency $\omega+\delta$ to that of a resonant pulse with $\mathrm{sech}(t/\alpha)$ envelope and cosine carrier wave.

$$F_0\,\mathrm{sech}\left(\frac{t}{\alpha+\delta}\right)\left[\cos(\omega t)-\frac{1}{(\alpha+\delta)\omega}\sin(\omega t)\tanh\left(\frac{t}{\alpha+\delta}\right)\right]$$
$$=F_0\,\mathrm{sech}\left(\frac{t}{\alpha}\right)\cos(\omega t). \tag{27}$$

Expanding the equation around $t=0$ and solving for δ one obtains

$$\delta=\omega\left(1-\frac{\sqrt{3+4n_c^2\pi^2+n_c^4\pi^4}}{3+n_c^2\pi^2}\right). \tag{28}$$

For the system under consideration the above equation predicted a shift in the carrier frequency of $\delta=1.17$ THz which is in very good agreement with the numerical result of 1.08 THz. It is also interesting to note that in the limit $n_c\to0$ sech-envelope pulses acquire a constant frequency shift of $\delta_{n_c\to0}=\omega-\omega/\sqrt{3}$.

C. Multilevel system dynamics

By extending the analysis beyond the two-level system, additional mechanisms governing population transfer came into play. These are, for example, resonance leaking, vibrational ladder climbing phenomena, or wave packets formation.

The multilevel system under consideration is the O···H···O moiety of acetylacetone. Therefore, the focus is on the laser driven H-atom transfer reaction. The molecular system is characterized by a double well potential energy surface (PES) with an effective transition state barrier of $\Delta E=28.33$ THz (0.12 eV). Details on the computation of the potential energy and dipole moment surfaces as well as of the eigenspectrum are given in Ref. [27]. The ground state doublet has an energy splitting of 3.48 THz, the second doublet, located 6.71 THz higher in energy, has a splitting of 5.49 THz, and the third one, 5.82 THz on top of the second, has a splitting of 5.97 THz. Both the eigenvalue spectrum and the selection rules suggest that because of the vibrational ladder climbing mechanism excited vibrational states may influence the ground state population dynamics.

Figure 7 is the multilevel analog of the two-level isomerization landscape shown in Fig. 5. Altogether 50 eigenstates have been included in the computation to span an energy range of more than 90 THz. An overall decrease of the isomerization efficiency from $P_2^2(t_{max})\approx1$ to $P_2^{50}(t_{max})=0.77$ is observed with the isomerization maximum occurring at $\omega=2.23$ THz. As in the two-level system most of the shift

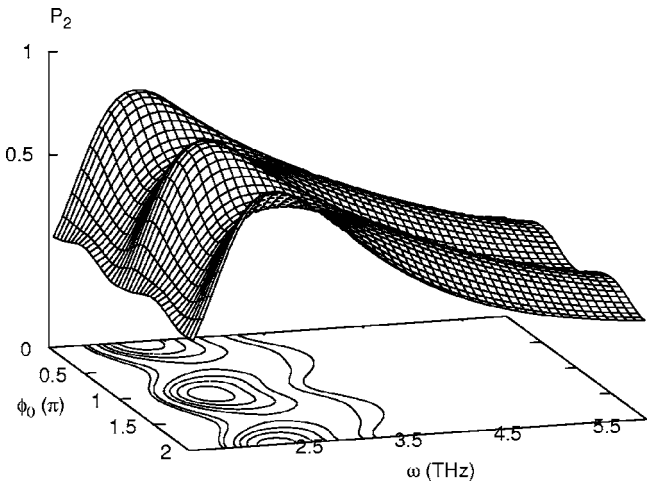

FIG. 7. CE phase sensitive dynamics in a multilevel system. Isomerization probability landscape for the H-transfer reaction in ACAC. The results are obtained by the numerical solution of Eq. (6) using the lowest 50 eigenstates of the 3D double well PES.

can be attributed to the change in the effective pulse frequency. However, to avoid a building up of the population in the strongly coupled third level the laser frequency is further shifted from resonance. The most interesting feature, however, is an increased sensitivity to the CE phase. The probability transfer landscape shows three distinct maxima located at $\phi=k\pi$ for $k=0,1,2$. In the previous section we have shown that in a two-level system the population transfer yield, i.e., the population remaining in the upper state of the system after the interaction with a pulse is almost insensitive to the CE phase. The origin of the multilevel phase sensitivity stems from the fact that in a two-level system the population transfer yield is not phase sensitive, but the population dynamics *during* the interaction with the laser field is CE phase sensitive. Figure 8 confronts the population evolution curves of the initial and final state, as well as the cumulative population of higher vibrational levels. The faster rate of population transfer occurs at peak fields strengths. The laser pulse with $\phi=0$, which is a variant of a single lobe pulse, induces maximum population transfer around the pulse center. The two shallow lobes on the wings have a minor influence on the dynamics. By contrast, the $\phi=\pi/2$ laser pulse has a double maxima structure which triggers a two step population transfer process. In the first step the population is transferred from the initial to the target state with maximum efficiency at the field maximum. At the center of the pulse the electric field is zero and therefore no population transfer occurs. Then the second lobe transfers the population from the already populated target state to the coupled third state with maximum efficiency at the second peak of the pulse. Consequently, at $\phi=\pi/2$ a minimum appears in the population of the target state, while the isomerization landscape acquires the three maxima structure.

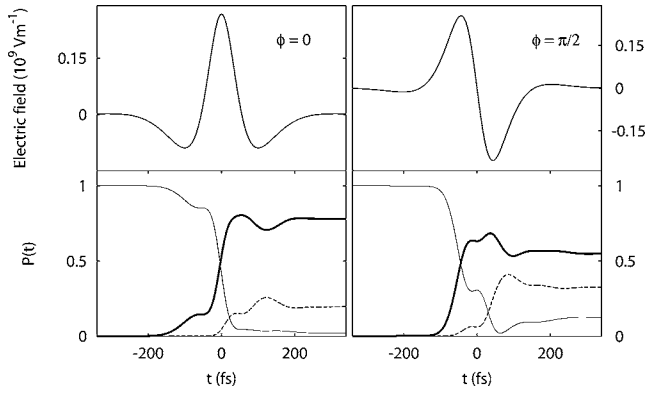

FIG. 8. CE phase sensitivity in a multilevel system: comparison of the laser fields ($n_c=0.25$, $\omega=2.2$ THz) and population dynamics in the 3D ACAC system. Ground state, $v=1$ (solid thin), target, $v=2$ (solid bold), and $v=3$ (dashed).

It is now straightforward to imagine a 0.25 pulse with $\phi=\pi/2$ capable of inducing a direct $v\rightarrow v\pm2$ transition, and indeed, a pulse with $\omega=1.46$ THz and $F_0=0.51\times10^9$ V m^{-1} triggers population transfer to $v=3$ with more than 60% efficiency. The analysis and optimization of such pulses are of interest, but are beyond the scope of the present contribution and shall be addressed separately.

VI. CONCLUSIONS

In the ultrashort pulse limit the definition of the electric field via the vector potential provides an accurate framework for studying laser driven dynamics in multilevel quantum systems. The goal of the presented work has been to refine previous researches on sub-one-cycle pulse dynamics, and to analyze different effects arising form the explicit inclusion of the finite pulse duration into the time-dependent Schrödinger equation. To that end we employed direct perturbation theory to analyze the dynamics of a simple two-level system under resonant excitation. The analysis is complemented by a more general analytical theory and numerical non-RWA simulations. In particular, the numerical approach allowed us to test the range of validity of the analytical results and to explore nonresonance and phase effects. Throughout the paper we employed sech-shaped laser pulses with $n_c=1.5$ down to 0.25 optical cycles within the width of the pulse.

Apart from an overall deviation from the Rabi-type dynamics we found specifically a shortening of the population inversion time scale inversely proportional to n_c^2. Moreover, we have shown that complete population transfer is unobtainable under resonant ultrashort pulse condition. Numerically the maximum population transfer yield at resonance has been estimated as $\kappa^2/4$, with κ being the electric field switching parameter.

Nonresonance effects have been studied numerically and it has been show that complete population inversion occurs at a frequency that is significantly redshifted from resonance. The frequency shift stems from the fact that the electric field switching term narrows the pulse width, i.e., effectively increases the pulse frequency. The observed redshift of the carrier frequency is hence a compensation for this effect. In the weak field regime the two-level system population inversion has proven to be almost insensitive to the variation of the CE phase. By contrast, the investigated multilevel system exhibits an increased CE phase sensitivity. That is due to the fact that a change in the CE phase from 0 to $\pi/2$ corresponds

to a shift from a single lobe pulse to a double lobe pulse, and each pulse lobe acts as an independent pump pulse. Hence a double peak pulse exchanges two vibrational quanta, while a virtually single lobe pulse with $\phi=0$ induces a $v \rightarrow v \pm 1$ transition.

An extension of the present approach to the laser control in the ultrashort domain is possible and would be desirable. This would include both methodological developments in the optimal control theory, for example, and system developments aimed at controlling more complicated phenomena. The presented analytical results on the population inversion dynamics are not restricted to the IR and can be extended to the uv region as long as $\kappa \leqslant 1$. In the recent strong field CE phase sensitive experiment of Niikura *et al.* [28] at 800 nm this situation corresponds to $n_c \geqslant 0.75$. As a matter of fact, few-cycle and sub-one-cycle laser pulses in the uv spectral region have been employed in quantum simulations of periodic electron circulation in a model Mg porphyrin [11,12]. The effects of the sub-cycle pulse duration on the effective shape of the laser pulse, however, have not been taken into account. These possibilities are topics of a forthcoming work.

ACKNOWLEDGMENTS

The author thanks I. Barth (Berlin), S. D. Bosanac (Zagreb), and J. Manz (Berlin) for assistance and stimulating discussions. This work has been supported by the Croatian Ministry of Science and Education under Project No. 0098033 and the Humboldt Foundation.

[1] T. Brabec and F. Krausz, Rev. Mod. Phys. **72**, 545 (2000).
[2] M. Drescher, M. Hentschel, R. Kienberger, G. Tempea, C. Spielmann, G. A. Reider, P. B. Corkum, and F. Krausz, Science **291**, 1923 (2001).
[3] P. M. Paul, E. S. Toma, P. Breger, G. Mullot, F. Augé, Ph. Balcou, H. G. Muller, and P. Agostini, Science **292**, 1689 (2001).
[4] A. Baltuška, Th. Udem, M. Uiberacker, M. Hentschel, E. Goulielmakis, Ch. Gohle, R. Holzwarth, V. S. Yakovlew, A. Scrinzi, T. W. Hänsch, and F. Krausz, Nature (London) **421**, 611 (2003).
[5] Z. Chang, Phys. Rev. A **70**, 043802 (2004).
[6] Z. Chang, Phys. Rev. A **71**, 023813 (2005).
[7] A. de Bohan, Ph. Antoine, D. B. Milošević, and B. Piraux, Phys. Rev. Lett. **81**, 1837 (1998).
[8] A. D. Bandrauk and N. H. Shon Phys. Rev. A **66**, 031401(R) (2002).
[9] *Laser Control and Manipulation of Molecules*, edited by A. D. Bandrauk, Y. Fujimura, and R. J. Gordon, ACS Symposium Series, Vol. 821 (ACS, Washington, 2002).
[10] N. Došlić, Y. Fujimura, L. Gonzalez, K. Hoki, D. Kroener, O. Kühn, J. Manz, and Y. Ohtsuki, in *Femtochemistry*, edited by F. C. DeSchryver, S. DeFeyter, and G. Schweitzer (VCH-Wiley, Berlin, 2001).
[11] I. Barth and J. Manz, Angew. Chem., Int. Ed. **45**, 2962 (2006).
[12] I. Barth, J. Manz, Y. Shigeta, and K. Yagi, J. Am. Chem. Soc. **128**, 7043 (2006).
[13] G. Tempea, M. Geissler, and T. Brabec, J. Opt. Soc. Am. B **16**, 669 (1999).
[14] G. Sansone, E. Benedetti, J.-P. Caumes, S. Stagira, C. Vozzi, M. Pascolini, L. Poletto, P. Villoresi, S. De Silvestri, and M. Nisoli, Phys. Rev. Lett. **94**, 193903 (2005).
[15] A. Gürtler, F. Robicheaux, M. J. J. Vrakking, W. J. van der Zande, and L. D. Noordam, Phys. Rev. Lett. **92**, 063901 (2004).
[16] C. Uiberacker and W. Jakubetz, J. Chem. Phys. **120**, 11532 (2004).
[17] C. Uiberacker and W. Jakubetz, J. Chem. Phys. **120**, 11540 (2004).
[18] Ch. Jirauschek, L. Duan, O. D. Múcke, F. X. Kärtner, M. Wegener, and U. Morgner, J. Opt. Soc. Am. B **22**, 2065 (2005).
[19] N. Došlić, O. Kühn, J. Manz, and K. Sundermann, J. Phys. Chem. A **102**, 9645 (1998).
[20] N. Došlić and O. Kühn, Chem. Phys. **255**, 247 (2000).
[21] L. Allen and J. H. Eberly, *Optical Resonance and Two-level Atoms* (Dover, New York, 1987).
[22] M. Holthaus and B. Just, Phys. Rev. A **49**, 1950 (1994).
[23] R. Parzński and M. Sobczak, J. Phys. B **37**, 743 (2004).
[24] D. Bonacci, S. D. Bosanac, and N. Došlić, Phys. Rev. A **70**, 043413 (2004).
[25] J. Rauch and G. Mourou, Proc. Am. Math. Soc. **134**, 851 (2006).
[26] G. M. Genkin, Phys. Rev. A **58**, 758 (1998).
[27] I. Matanović and N. Došlić, J. Phys. Chem. A **109**, 4185 (2005).
[28] H. Niikura, D. M. Villeneuve, and P. B. Corkum, Phys. Rev. A **73**, 021402(R) (2006).